

Anisotropic Anomalous High-Harmonic Generation from Time-Reversal Symmetry Broken Weyl Semimetal

Amar Bharti,¹ M. S. Mrudul,¹ and Gopal Dixit^{1,*}

¹*Department of Physics, Indian Institute of Technology Bombay, Powai, Mumbai 400076, India*

(Dated: December 6, 2021)

Weyl semimetals are promising quantum materials that offer unique topological properties. Lately, it has been shown that laser-driven electron dynamics have characteristic signatures in two-dimensional and three-dimensional Dirac semimetals. The transition from Dirac to Weyl semimetal requires the breaking of either inversion or time-reversal symmetry. The present work shows that the laser-driven electron dynamics in a Weyl semimetal with broken time-reversal symmetry has unique features in its high-harmonic spectrum. We demonstrate that the anomalous current due to the Berry curvature results in odd harmonics, which encode the symmetry and magnitude of the Berry curvature. Our findings of the anisotropic anomalous current in Weyl semimetal is analogous to the anisotropic anomalous Hall effect. To support our findings, high-order harmonics generated by linearly and circularly polarised pulses are discussed.

Discoveries of topological materials, such as topological insulators, Dirac and Weyl semimetals, have revolutionised contemporary physics [1, 2]. Moreover, these materials hold promises for upcoming technologies based on quantum science and electronics [3–5]. One of the remarkable properties of these materials is the robustness of the electronic states against perturbations, which has catalysed a plethora of interesting phenomena [6–8]. Methods based on light-matter interaction play a pivotal role in probing and understanding various exotic properties of these topological materials [9–11].

If one increases the intensity of the light significantly, various interesting perturbative and non-perturbative nonlinear processes occur in the matter. High-harmonic generation (HHG) is one such nonlinear process in which radiation of integer multiples of the incident light's frequency is emitted [12, 13]. Moreover, numerous static and dynamic properties of the matter can be extracted by analysing the emitted radiation during HHG [14–23]. In recent years, topological materials have turned out to be the centre of attention for HHG [24–28]. It is experimentally found that the bulk and the topological surface play different roles during HHG from a topological insulator [29]. The interplay of time-reversal symmetry protection and spin-orbit coupling in a topological insulator leads to anomalous dependence of harmonic yield on the polarisation of the driving laser [30]. Berry curvature plays an important role in determining the behaviour of high-harmonic spectra in both cases. In three-dimensional Dirac semimetal, coherent dynamics of the Dirac electrons plays the central role in HHG [31, 32]. Moreover, it has been reported that the nonlinear responses of the three- and two-dimensional Dirac semimetals are significantly different [33]. In all cases, time-reversal symmetry (TRS) is inherently preserved in topological insulators and Dirac semimetal. Therefore, it is natural to envision exploring how the breaking of the TRS affects HHG from topological materials and is the main focus of the present work.

Weyl semimetal (WSM) consists of the topologically protected degenerate points, known as Weyl points, which can be seen as the monopoles of the Berry curvatures in momentum space [2]. This makes WSM one of the most exotic gapless systems. Weyl semimetal can be formed either by breaking time-reversal or inversion symmetry of the corresponding Dirac semimetal phase, either case results in non-zero Berry curvature [8]. In 2015, the first WSM was realised experimentally in transition-metal monpnictides, which form the class of nonmagnetic WSM with broken inversion-symmetry [34–36]. Later, three groups have shown the evidence of magnetic WSM in ferromagnetic materials with broken TRS experimentally [37–39].

Present work focuses on addressing some crucial questions such as how TRS breaking and resultant modifications in Berry curvature affect HHG, the role of the behaviour and parity of the Berry curvature, and how the separations of the Weyl points influence HHG in WSM. In the following, we will demonstrate that non-zero Berry curvature in TRS-broken WSM leads to anomalous current in a direction perpendicular to the electric field and anomalous odd harmonics – analogous to anomalous Hall effect. Moreover, we will show that the directions of the emitted anomalous odd harmonics are related to the nature of the Berry curvature's components. Recently, HHG from an inversion-symmetry broken WSM was explored experimentally in which linearly polarised pulse leads to the generation of even harmonics, related to non-zero Berry curvature [40]. Our findings are in contrast to previously reported works where Berry curvature mediated anomalous electron's velocity leads to the generation of even harmonics [16, 18, 41, 42].

The Hamiltonian corresponding to WSM with broken TRS can be written as [43]

$$\mathcal{H}(\mathbf{k}) = \mathbf{d}(\mathbf{k}) \cdot \boldsymbol{\sigma} = d_1(\mathbf{k})\sigma_x + d_2(\mathbf{k})\sigma_y + d_3(\mathbf{k})\sigma_z. \quad (1)$$

Here, $\boldsymbol{\sigma}$ is the Pauli vector and $d_1 = t_x\{\cos(k_x a) - \cos(k_0 a)\} + t_y\{\cos(k_y b) - 1\} + t_z\{\cos(k_z c) - 1\}$, $d_2 =$

$t_y \sin(k_y b)$ and $d_3 = t_z \sin(k_z c)$ with $(\pm k_0, 0, 0)$ as the positions of Weyl points, $t_{x,y,z}$ as hopping parameters and a, b, c are lattice parameters. Here, we assume ferromagnetic WSM with tetragonal crystal structure, i.e., $a = b \neq c$ [44]. $a = b = 3.437 \text{ \AA}$, $c = 11.646 \text{ \AA}$ and $t_x = 1.88 \text{ eV}$, $t_y = 0.49 \text{ eV}$, $t_z = 0.16 \text{ eV}$ are considered. The parameters used here are in accordance with the ones used in Ref. [45]. It is easy to see that the above Hamiltonian exhibits TRS breaking, i.e., $\hat{T}^\dagger \mathcal{H}(-\mathbf{k}) \hat{T} \neq \mathcal{H}(\mathbf{k})$. However, $\hat{P}^\dagger \mathcal{H}(-\mathbf{k}) \hat{P} = \mathcal{H}(\mathbf{k})$ ensures that inversion symmetry is preserved. Here, \hat{T} and \hat{P} are the time-reversal symmetry and inversion symmetry operators, respectively.

After diagnosing the above Hamiltonian, energy dispersion can be obtained as $\mathcal{E}_\pm = \pm |\mathbf{d}(\mathbf{k})| = \pm \sqrt{d_1^2 + d_2^2 + d_3^2}$. We have considered $k_0 = 0.2 \text{ rad/au}$. The corresponding band-structure in $k_z = 0$ plane is plotted in Fig. S1.

Interaction of the laser with the WSM is modelled using semiconductor-Bloch equations in the Houston basis as discussed in Refs. [17, 46]. Within this formalism, current at any time can be written as

$$\mathbf{J}(\mathbf{k}, t) = \sum_{m,n} \rho_{mn}^{\mathbf{k}}(t) \mathbf{p}_{mn}^{\mathbf{k}_t}, \quad (2)$$

where $\mathbf{k}_t = \mathbf{k} + \mathbf{A}(t)$ with $\mathbf{A}(t)$ as the vector potential of the laser, and $\rho_{mn}^{\mathbf{k}}(t)$ is the density matrix at time t . Here, $\mathbf{A}(t)$ is related to its electric field $\mathbf{E}(t)$ as $\mathbf{E}(t) = -\partial \mathbf{A}(t) / \partial t$. $\mathbf{p}_{nm}^{\mathbf{k}_t}$ is momentum matrix element and calculated as $\mathbf{p}_{nm}^{\mathbf{k}_t} = \langle n, \mathbf{k}_t | \nabla_{\mathbf{k}_t} \mathcal{H}_{\mathbf{k}_t} | m, \mathbf{k}_t \rangle$. By performing the integral over entire Brillouin zone and taking Fourier transform (\mathcal{FT}), high-harmonic spectrum is simulated as

$$\mathcal{I}(\omega) = \left| \mathcal{FT} \left(\frac{d}{dt} \left[\int_{BZ} \mathbf{J}(\mathbf{k}, t) d\mathbf{k} \right] \right) \right|^2. \quad (3)$$

Figure 1 presents high-harmonic spectra corresponding to linearly polarised pulse. When the pulse is polarised along x direction, odd harmonics are generated along the laser polarisation as evident from Fig. 1(a). However, results become interesting when the pulse is polarised along y or z direction. In both cases, odd harmonics are generated along the laser polarisation. Moreover, anomalous odd harmonics along perpendicular directions are also generated. As reflected from Figs. 1(b) and (c), when laser is along y or z direction, odd harmonics along z or y direction are generated, respectively. However, the yield of the anomalous harmonics is relatively weaker in comparison to the parallel harmonics. Our results are in contrast to the recent findings for inversion-symmetry breaking WSM, where odd and even harmonics are observed [40]. Moreover, it has been concluded that the appearance of the even harmonics is related to the spike-like Berry curvatures in WSM [40].

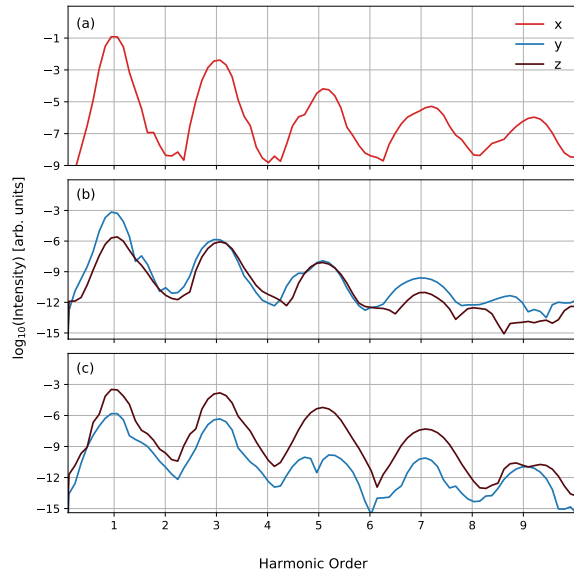


FIG. 1. High-harmonic spectra corresponding to a linearly polarised pulse. The pulse is polarised along (a) x , (b) y , and (c) z directions. Driving pulse is $\simeq 100 \text{ fs}$ long with intensity $1 \times 10^{11} \text{ W/cm}^2$, and wavelength 3.2 \mu m . Decoherence time of 1.5 fs is added phenomenologically in semiconductor Bloch equations.

To understand why linear pulse leads to parallel and anomalous odd harmonics, and how these findings are related to TRS breaking in WSM, let us employ semiclassical equation of Bloch electrons in an external electric field $\mathbf{E}(t)$. Within this approach, expression of the anomalous current is written as $\mathbf{J}_\Omega(t) = -\mathbf{E}(t) \times \int \Omega_\mu(\mathbf{k}) \rho_\mu(\mathbf{k}, t) d\mathbf{k}$ with Ω_μ and $\rho_\mu(\mathbf{k}, t)$ as the Berry curvature and band-population of μ^{th} energy band, respectively [41]. We can assume that the initial band population is symmetric under inversion as $\rho(\mathbf{k}, 0) = \rho(-\mathbf{k}, 0)$. In the presence of laser, momentum of an electron changes as $\mathbf{k}_t = \mathbf{k} + \mathbf{A}(t)$, which leads to the change in the band population as $\rho(\mathbf{k}, t) = \rho(\mathbf{k}_t, 0)$. Under time-translation of the laser $t \rightarrow t + T/2$, anomalous current can be expressed as

$$\begin{aligned} \mathbf{J}_\Omega(t + T/2) &= -\mathbf{E}(t + T/2) \times \int \Omega_\mu(\mathbf{k}) \rho_\mu(\mathbf{k}_t + T/2, 0) d\mathbf{k} \\ &= \mathbf{E}(t) \times \int \Omega_\mu(\mathbf{k}) \rho_\mu(\mathbf{k} - \mathbf{A}(t), 0) d\mathbf{k} \\ &= \mathbf{E}(t) \times \int \Omega_\mu(\mathbf{k}) \rho_\mu(\mathbf{k}_t, 0) d\mathbf{k} \\ &= -\mathbf{J}_\Omega(t). \end{aligned} \quad (4)$$

In the above equations, we have used $\mathbf{E}(t + T/2) = -\mathbf{E}(t)$ and $\mathbf{A}(t + T/2) = -\mathbf{A}(t)$, $\rho(\mathbf{k}, 0) = \rho(-\mathbf{k}, 0)$; and changed the dummy variable $\mathbf{k} \rightarrow -\mathbf{k}$ in the integral. Also, Berry curvature for an inversion-symmetric system with broken TRS fulfils $\Omega(\mathbf{k}) = \Omega(-\mathbf{k})$.

The contribution of $\mathbf{J}_\Omega(t)$ to the n^{th} harmonic is given by $\mathbf{J}_\Omega^n(\omega) \propto \int_{-\infty}^{\infty} \mathbf{J}_\Omega(t) e^{in\omega t} dt$. By changing $t \rightarrow t + T/2$ in the integral, we obtain $\mathbf{J}_\Omega^n(\omega) \propto \int_{-\infty}^{\infty} \mathbf{J}_\Omega(t + T/2) e^{in\omega(t+T/2)} dt = -e^{in\pi} \int_{-\infty}^{\infty} \mathbf{J}_\Omega(t) e^{in\omega t} dt$, which implies that only odd harmonics are allowed as $\exp(in\pi) = -1$. Therefore, TRS broken systems lead to anomalous odd harmonics, which is in contrast to the case of time-reversal symmetric systems with broken-inversion symmetry where anomalous current leads to the generation of even harmonics [16, 18, 41, 42].

In order to discern the directions of the anomalous current, we need to understand the distinct role of the Berry curvature's components, which is written as $\mathbf{\Omega}(\mathbf{k}) = \Omega_{k_x}(\mathbf{k})\hat{e}_{k_x} + \Omega_{k_y}(\mathbf{k})\hat{e}_{k_y} + \Omega_{k_z}(\mathbf{k})\hat{e}_{k_z}$. The expressions of the Berry curvature's components corresponding to Hamiltonian in Eq. (1) are given in the supplementary material. The direction of the anomalous current is given by $\mathbf{E} \times \mathbf{\Omega}$ and the integral is performed over entire Brillouin zone. Moreover, \mathbf{E} is a function of time and $\mathbf{\Omega}$ is function of \mathbf{k} , so their product does not change the parity.

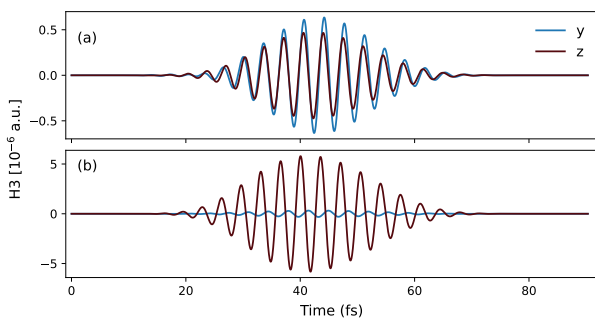


FIG. 2. Third harmonic in time domain. When the pulse is linearly polarised along (a) y direction and (b) z direction. The driving pulse has same parameters as in Fig. 1.

If the laser is polarised along x direction, then it is straightforward to see that anomalous current along y and z directions turn out to be zero as Ω_{k_y} and Ω_{k_z} are odd functions in two directions. On the other hand, Ω_{k_x} is an even function in all the directions, contributing to the anomalous current when the laser is polarised along y or z directions. This is consistent with our numerical results of the harmonics as shown in Fig. 1.

To see whether the parallel and anomalous harmonics are in phase or not, we investigate third harmonic (H3) in time domain. When the laser is polarised along y direction, H3 along y and z directions is in phase as evident from Fig. 2(a). However, it becomes out of phase in the case of z polarised pulse. The reason behind in phase or out-of-phase of H3 can be attributed to the sign of $\mathbf{J}_\Omega(t) \propto \int \mathbf{E}(t) \times \mathbf{\Omega}(\mathbf{k}) d\mathbf{k}$, which yields positive (negative) sign when laser is along $y(z)$ direction.

To strengthen our findings about the generation of the anomalous harmonics and their relation with the form

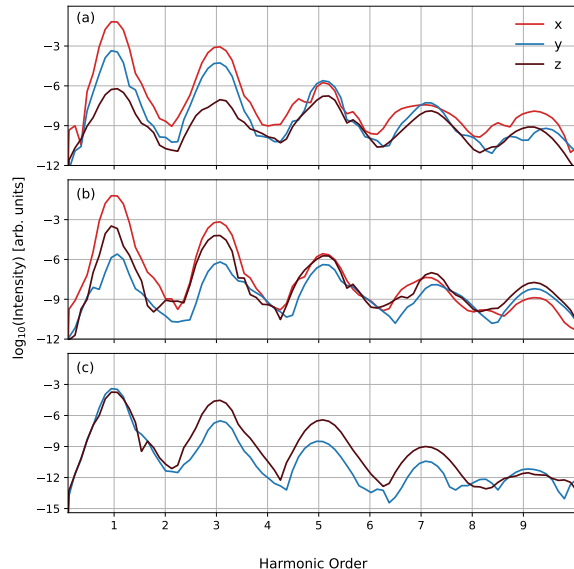


FIG. 3. High-harmonic spectra generated by right-handed circularly polarised pulse in (a) $x - y$, (b) $x - z$, and (c) $y - z$ planes. The parameters of the laser and decoherence time are same as given in Fig. 1.

and parity of the Berry curvature's component, high-harmonic spectra generated by circularly polarised pulse are presented in Fig. 2. In agreement with the two-fold rotation symmetry of the Hamiltonian, only odd harmonics are generated. When the pulse is in $x - y$ plane, odd harmonics along x and y directions are generated as x and y components of the driving electric field are non-zero. Moreover, due to the non-zero y component of the driving field, anomalous odd harmonics are generated along z direction [see Fig. 2(a)]. In this case, the mechanism is same as it was in the case of linearly polarised pulse along y direction. Same is true in the case of circularly polarised pulse in $x - z$ plane. In this case, parallel odd harmonics are generated along x and z directions, whereas anomalous odd harmonics are generated along y direction [see Fig. 2(b)]. However, when the pulse is polarised in $y - z$ plane, only parallel harmonics along y and z directions are generated, and no anomalous harmonics along x direction are generated. This is expected due to even and odd natures of the Ω_{k_x} and Ω_{k_z}/k_z (see supplementary information).

After establishing the role of the components of the Berry curvature and its parity, let us explore how their strengths affect the yield of the anomalous harmonics. We know that the magnitude of the anomalous current depends on $\mathbf{E} \times \mathbf{\Omega}$. Moreover, the magnitude of the Berry curvature's components depend on k_0 (see supplementary information). Therefore, as we change the value of k_0 from 0.2 to 0.3, the strength of the Berry curvature's

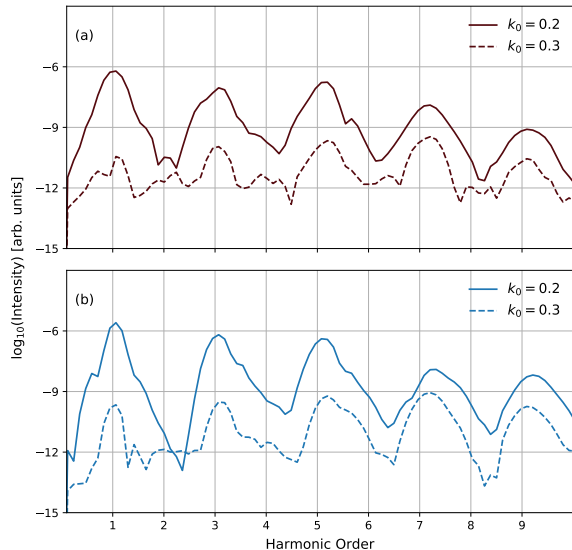


FIG. 4. Comparison of the anomalous high-harmonic yield for different values of $k_0 = 0.2$ and 0.3 rad/au. Odd anomalous harmonics along (a) z direction when polarisation of the pulse is in $x - y$ plane, and (b) y direction when polarisation of the pulse is in $x - z$ plane. k_0 is proportional to the distance between the two Weyl points.

components reduces, which lead to the reduction in the anomalous current's strength. Fig. 4 presents a comparison of the yield of the anomalous harmonics for two different values of k_0 . In the case of circularly polarised pulse in $x - y$ plane, the anomalous harmonics along z direction reduces drastically as we change k_0 from 0.2 to 0.3 rad/au [see Fig. 4(a)]. The same is true for the pulse in $x - z$ plane and anomalous harmonics along y direction [see Fig. 4(b)]. Therefore, the yield of the anomalous harmonics reduces drastically as the value of k_0 increased from 0.2 to 0.3 rad/au. Similar conclusions can be drawn in the case of HHG from linearly polarised pulse (see Fig. S3). However, the yield of the parallel harmonics is insensitive to the change in the value of k_0 (see Figs. S4 and S5). Our findings are similar to anisotropic anomalous hall effect in which the magnitude of the current depends on the integral of the Berry curvature [47].

In summary, we have investigated the role of TRS breaking in strong-field driven HHG. For this purpose, inversion symmetric Weyl semimetal with broken TRS is considered. It has been found that unlike in a system without inversion symmetry, where Berry curvature results in anomalous even-harmonics, the anomalous current results in odd harmonics in a TRS broken Weyl semimetal. The anomalous harmonics are anisotropic in nature, and appear only when the driving laser has non-zero components along y or z direc-

tion. The anisotropic nature of the anomalous harmonics (current) is attributed to the reflection symmetries of the Berry curvature's components corresponding to Weyl semimetal. Moreover, the strength of the anomalous current scales with the strength of the Berry curvature. Present work opens new avenue for studying strong-field driven electron dynamics and HHG in systems with broken TRS, such as exotic magnetic and topological materials.

* gdixit@phy.iitb.ac.in

- [1] M. Z. Hasan and C. L. Kane, *Revs. Mod. Phys.* **82**, 3045 (2010).
- [2] N. Armitage, E. Mele, and A. Vishwanath, *Revs. Mod. Phys.* **90**, 015001 (2018).
- [3] B. Keimer and J. E. Moore, *Nature Physics* **13**, 1045 (2017).
- [4] N. Sirica and R. Prasankumar, *Nature Materials* **20**, 283 (2021).
- [5] Y. Tokura, M. Kawasaki, and N. Nagaosa, *Nature Physics* **13**, 1056 (2017).
- [6] X.-L. Qi and S.-C. Zhang, *Revs. Mod. Phys.* **83**, 1057 (2011).
- [7] J. E. Moore, *Nature* **464**, 194 (2010).
- [8] B. Yan and C. Felser, *Annual Review of Condensed Matter Physics* **8**, 337 (2017).
- [9] D. N. Basov, R. D. Averitt, and D. Hsieh, *Nature Materials* **16**, 1077 (2017).
- [10] C. Bao, P. Tang, D. Sun, and S. Zhou, *Nature Reviews Physics*, 1 (2021).
- [11] J. McIver, D. Hsieh, H. Steinberg, P. Jarillo-Herrero, and N. Gedik, *Nature Nanotechnology* **7**, 96 (2012).
- [12] S. Ghimire, A. D. DiChiara, E. Sistrunk, P. Agostini, L. F. DiMauro, and D. A. Reis, *Nature Physics* **7**, 138 (2011).
- [13] S. Ghimire and D. A. Reis, *Nature Physics* **15**, 10 (2019).
- [14] T. T. Luu, M. Garg, S. Y. Kruchinin, A. Moulet, M. T. Hassan, and E. Goulielmakis, *Nature* **521**, 498 (2015).
- [15] M. Mrudul and G. Dixit, *Physical Review B* **103**, 094308 (2021).
- [16] O. Schubert, M. Hohenleutner, F. Langer, B. Urbaneck, C. Lange, U. Huttner, D. Golde, T. Meier, M. Kira, S. W. Koch, and R. Huber, *Nature Photonics* **8**, 119 (2014).
- [17] M. Mrudul, Á. Jiménez-Galán, M. Ivanov, and G. Dixit, *Optica* **8**, 422 (2021).
- [18] M. Hohenleutner, F. Langer, O. Schubert, M. Knorr, U. Huttner, S. W. Koch, M. Kira, and R. Huber, *Nature* **523**, 572 (2015).
- [19] B. Zaks, R. B. Liu, and M. S. Sherwin, *Nature* **483**, 580 (2012).
- [20] A. Pattanayak, G. Dixit, et al., *Physical Review A* **101**, 013404 (2020).
- [21] F. Langer, C. P. Schmid, S. Schlauderer, M. Gmitra, J. Fabian, P. Nagler, C. Schüller, T. Korn, P. G. Hawkins, J. T. Steiner, et al., *Nature* **557**, 76 (2018).
- [22] M. S. Mrudul, N. Tancogne-Dejean, A. Rubio, and G. Dixit, *npj Computational Materials* **6**, 1 (2020).
- [23] M. S. Mrudul, A. Pattanayak, M. Ivanov, and G. Dixit, *Physical Review A* **100**, 043420 (2019).

- [24] J. Reimann, S. Schlauderer, C. Schmid, F. Langer, S. Baierl, K. Kokh, O. Tereshchenko, A. Kimura, C. Lange, J. Gdde, *et al.*, *Nature* **562**, 396 (2018).
- [25] R. Silva, A. Jimnez-Galn, B. Amorim, O. Smirnova, and M. Ivanov, *Nature Photonics* **13**, 849 (2019).
- [26] Y. Bai, F. Fei, S. Wang, N. Li, X. Li, F. Song, R. Li, Z. Xu, and P. Liu, *Nature Physics* **17**, 311 (2021).
- [27] D. Bauer and K. K. Hansen, *Physical Review Letters* **120**, 177401 (2018).
- [28] R. M. Dantas, Z. Wang, P. Surwka, and T. Oka, *Physical Review B* **103**, L201105 (2021).
- [29] C. P. Schmid, L. Weigl, P. Grssing, V. Junk, C. Gorini, S. Schlauderer, S. Ito, M. Meierhofer, N. Hofmann, D. Afanasiev, *et al.*, *Nature* **593**, 385 (2021).
- [30] D. Baykusheva, A. Chacn, J. Lu, T. P. Bailey, J. A. Sobota, H. Soifer, P. S. Kirchmann, C. Rotundu, C. Uher, T. F. Heinz, *et al.*, *Nano Letters* (2021).
- [31] S. Kovalev, R. M. Dantas, S. Germanskiy, J.-C. Deinert, B. Green, I. Ilyakov, N. Awari, M. Chen, M. Bawatna, J. Ling, *et al.*, *Nature Communications* **11**, 1 (2020).
- [32] B. Cheng, N. Kanda, T. N. Ikeda, T. Matsuda, P. Xia, T. Schumann, S. Stemmer, J. Itatani, N. Armitage, and R. Matsunaga, *Physical Review Letters* **124**, 117402 (2020).
- [33] J. Lim, Y. S. Ang, F. J. G. de Abajo, I. Kaminer, L. K. Ang, and L. J. Wong, *Physical Review Research* **2**, 043252 (2020).
- [34] S.-Y. Xu, N. Alidoust, I. Belopolski, Z. Yuan, G. Bian, T.-R. Chang, H. Zheng, V. N. Strocov, D. S. Sanchez, G. Chang, *et al.*, *Nature Physics* **11**, 748 (2015).
- [35] S.-Y. Xu, I. Belopolski, N. Alidoust, M. Neupane, G. Bian, C. Zhang, R. Sankar, G. Chang, Z. Yuan, C.-C. Lee, *et al.*, *Science* **349**, 613 (2015).
- [36] B. Lv, H. Weng, B. Fu, X. P. Wang, H. Miao, J. Ma, P. Richard, X. Huang, L. Zhao, G. Chen, *et al.*, *Physical Review X* **5**, 031013 (2015).
- [37] N. Morali, R. Batabyal, P. K. Nag, E. Liu, Q. Xu, Y. Sun, B. Yan, C. Felser, N. Avraham, and H. Beidenkopf, *Science* **365**, 1286 (2019).
- [38] D. Liu, A. Liang, E. Liu, Q. Xu, Y. Li, C. Chen, D. Pei, W. Shi, S. Mo, P. Dudin, *et al.*, *Science* **365**, 1282 (2019).
- [39] I. Belopolski, K. Manna, D. S. Sanchez, G. Chang, B. Ernst, J. Yin, S. S. Zhang, T. Cochran, N. Shumiya, H. Zheng, *et al.*, *Science* **365**, 1278 (2019).
- [40] Y.-Y. Lv, J. Xu, S. Han, C. Zhang, Y. Han, J. Zhou, S.-H. Yao, X.-P. Liu, M.-H. Lu, H. Weng, *et al.*, *Nature Communications* **12**, 1 (2021).
- [41] H. Liu, Y. Li, Y. S. You, S. Ghimire, T. F. Heinz, and D. A. Reis, *Nature Physics* **13**, 262 (2017).
- [42] T. T. Luu and H. J. Wrner, *Nature Communications* **9**, 916 (2018).
- [43] M. Z. Hasan, S.-Y. Xu, I. Belopolski, and S.-M. Huang, *Annual Review of Condensed Matter Physics* **8**, 289 (2017).
- [44] B. Meng, H. Wu, Y. Qiu, C. Wang, Y. Liu, Z. Xia, S. Yuan, H. Chang, and Z. Tian, *APL Materials* **7**, 051110 (2019).
- [45] F. Nematollahi, S. A. O. Motlagh, J.-S. Wu, R. Ghimire, V. Apalkov, and M. I. Stockman, *Physical Review B* **102**, 125413 (2020).
- [46] I. Floss, C. Lemell, G. Wachter, V. Smejkal, S. A. Sato, X. M. Tong, K. Yabana, and J. Burgdrfer, *Physical Review A* **97**, 011401 (2018).
- [47] H.-Y. Yang, B. Singh, J. Gaudet, B. Lu, C.-Y. Huang, W.-C. Chiu, S.-M. Huang, B. Wang, F. Bahrami, B. Xu, *et al.*, *Physical Review B* **103**, 115143 (2021).